Transactions of the Nigerian Association of Mathematical Physics
Volume 15, (April –June, 2021 Issue), pp127 – 132

INFLUENCE OF DEPOSITION CYCLES ON SYNTHESIS AND CHARACTERIZATION OF SNS/SNO_2 MATERIAL FOR SOLAR CELL APPLICATION VIA SILAR METHOD

[1]Okunzuwa I.S. and [2]Egwunyenga N. Josephine

[1]Department of Physics, University of Benin
[2]Department of Science Laboratory Technology, Delta State Polytechnic Ogwashi-Uku

Abstract

In this study, SnS/SnO_2 heterojunction thin were successfully coated on glass subtract at room temperature using successors ionic layer absorption and reaction (SILAR) method.

Variation in SILAR cycle which is important in SILAR management, were used to obtain SnS/SnO_2 heterojunction thin films. X -ray diffraction spectroscopy (XRD), scanning Electron microscopy (SEM)/ Energy spread x- ray spectroscopy (EDX) was used to examine the changes in the structure with the SILAR cyclus, between the range of 20, 25, 30, 35 and 40 cycles respectively. Because at the investigations, it was found that SnS/ SnO_2 thin films improved, the crystal structure improved and the SEM/ EDX, electrical and optical properties supported this results.

INTRODUCTION

Fabrication of environmentally friendly semiconductor materials such as tin sulfide and tin Oxide is actually possible by employing SILAR method for solar energy application. SnS, which belongs to IV – VI group semiconductors has a direct energy band gap of 1.3 eV, and has high absorption coefficient, which makes it a good candidate for absorption layer.

SnO_2 with a wide band gap of (3 .8eV) is seen as one of the well known transparent conducting Oxides and a good window or buffer layer materials for heterojunction solar energy application [1] owing to its high optical transparency (T>85%) in the visible region, low electrical resistance and good thermal resistance, Tin Oxide has majorly been used in large number of optoelectric devices such as light emitting diodes, as electrode and buffer layer materials in solar cells, transparent filled effect transistors etc, [2]. Tin Oxide ($SnO_{2)}$ is considered as one of the most important n-type semiconductor[3]. Rama et al, deposited tin oxide thin films uniformly onto a glass substrate by successive ionic layer adsorption reaction (SILAR) method on using diamine as a complexing agent. The energy band gap of the deposited films was around 3.85 eV while the electrical conductivity between $4.23 \times 10^8\ \Omega$cm – $11.83 \times 10^8\ \Omega$cm [2].

So far the highest solar conversion efficiency of 1.3% in SnS- related heterojunction devises was obtained from Cds/SnS heterojunction [4]. However, SnS and $Sn0_2$ has an advantage for solar energy application which is, the constituent elements are relatively economical, abundant and non toxic. To avoid toxicity of CdS layer, however SnS is used as $Sn0_2$ heterojunction partner. fabricated SnS/SnO_2 heterostructure by a combination of chemical bath deposition and spray pyrolysis techniques. So far, no studies on the fabrication of SnS/SnO heterojunction thin films by SILAR method route have been reported. Therefore, the effect of SILAR cycles on the fabrication of SnS/SnO_2 heterojunction Thin Film for solar energy application is evaluated and reported in this work.

Experimental procedure

In the deposition of SnS/SnO, the following precursor were used, 0.1 M of tin (II) chloride dihydrate ($SnCl_2.2H_2O$) was used to form the cationic precursor solution and the anionic precursor solution was 0.01 M Thioacetamide (C_2H_5NS).

Correspondence Author: Okunzuwa I.S., Email: ikponmwosa.okunzuwa@uniben.edu, Tel: +2348063034388, +2348067957485 (ENJ)

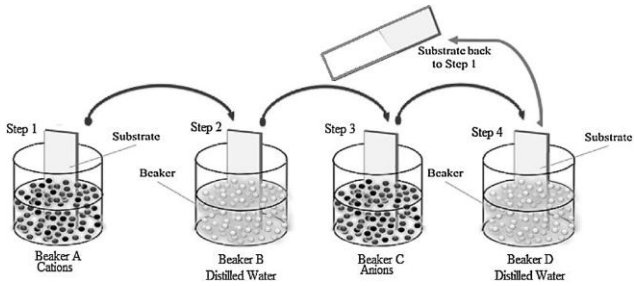

Figure 1: A Schematic diagram of SILAR deposition technique

The setup was made up of four sets of 50 ml beakers labeled A, B, C, and D. Beaker A contained tin (II) chloride dihydrate ($SnCl_2.2H_2O$) solution, beaker B contained distilled water, beaker C contained Thioacetamide (C_2H_5NS)/potassium hydroxide (KOH) solution and beaker D contained distilled water as well (see figure 1). A well cleaned glass substrate which was cleaned with acid, in succession with distilled water and acetone was immersed in a cationic precursor solution tin (II) chloride dihydrate ($SnCl_2.2H_2O$) for 10 s, for adsorption of tin ions on the substrate surface. The substrate was rinsed in distilled water for 5 s to remove loosely bound ions of Sn^{2+}. Then, the substrate was immersed in the anionic precursor solution Thioacetamide (C_2H_5NS)/potassium hydroxide (KOH). for 10 s to form a layer of SnS/SnO materials. Rinsing the substrate again in distilled water for 5 s to separate out the unreached species, thus one SILAR cycle of SnS deposition was completed. Such cycles were repeated at room temperature for different variations. The deposition cycles was varies as the parameters for characterization in the process of the synthesis from 20 cycles, 25 cycles, 30 cycles, 35 cycles, and 40 cycles, precursor pH 7.0, and precursor temperature (room) and every other parameter were kept constant. The synthesis of SnS/SnO superlattice films, tin oxide (SnO) was first deposited on the glass substrate dry in the oven for 30 minute and tin sulphide (SnS) was deposited on the grown SnO films to make SnS/SnO superlattice films and it was repeated for a different parameter for characterization.

Characterization Techniques

Some already existing techniques were used to ascertain the properties of the deposited films. The characterization provides the knowledge of the chemical composition, crystal structure, crystallite size, surface morphology, band gap energy, optical absorption, transmittance and absorbance of the deposited film. The chemical compositions of the thin films deposited in this work were determined by: phase identification of the films performed by means of X-ray diffraction (XRD) using Bruker D8 Advance X-ray diffractometer with Cu-Kα line (λ= 1.54056 Å) in 2θ range from 10° - 90°The morphology and the size of the prepared particles were investigated with scanning electron microscope (SEM) model A-VPSE G3 with an acceleration voltage of 20 kV and the magnification range from 200x to1000x andthe optical properties of the films deposited were examined for their absorbance and transmittance at normal incidence by using a UV-visible spectrophotometer. 756S UV-Visible Spectrophotometer, four-point probe (Model T345) and Scanning Electron Microscopy

Results and Discussions

The XRD patterns of SnS/SnOmaterial deposited on glass substrate at different cycles is shown in figure 2. At 30 cycles, the significant peak was found at 2θ values of 31.6252^o which correspond to the face-centered cubic crystal structure (FCC) with orientations along (111) plane were identified as SnS and (300) as SnO. The lattice constant was given as $\alpha = 4.89567$Å. The several peaks observed confirm that SnS/SnO material deposited by SILAR method were observed to be used as a hole conductor in dye-sensitized solar cells (see table 1). The average crystallite sizes were calculated according to the full width at half maxima (FWHM) of the diffraction peaks using Debye-Scherrer equation. The XRD pattern showed that the films were polycrystalline in nature with cubic structure.

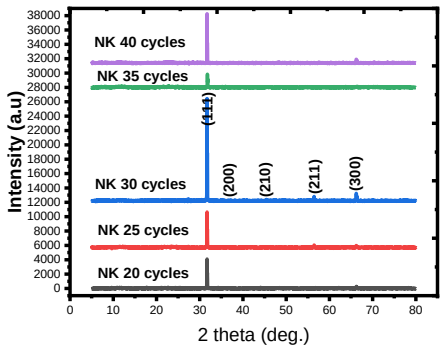

Figure 2: XRD pattern of SnS/SnO material deposited at different cycles

Table 1: Structural values for the **SnS/SnO** at different cycles.

Sample	2θ (degree)	Spacing d(Å)	Lattice constant (Å)	FWHM, β	Hkl	Crystallite Size,D (nm)	Dislocation density, δ m^2
SnS/SnO	**31.6252**	**2.8265**	**4.89567**	**0.18517**	111	**0.77825**	**5.0061**
	37.2522	2.4114	4.82295	0.20958	200	0.69815	6.2312
	45.4181	1.9950	3.99016	0.14800	210	1.01560	2.9450
	56.4319	1.6290	3.64266	0.22584	211	0.69676	6.1985
	66.2448	1.4095	3.45264	0.22499	300	0.73587	5.5789

Figure 2 shows the material deposited at different deposition cycles (20 cycles – 40 cycles) displays the surface morphological images of all the deposited materials (SnS/SnO at 200 nm magnification. It can be seen that large crystals packers composed of various sizes were observed for 20 cycles which consist of uneveningly shaped and not firmly packed particles while for 25 and 30 cycles, the crystallite size is larger compare to the material deposited at 35 cycles.The material deposited shows that the particles are agglomerated which resulted from the formation of large grains.

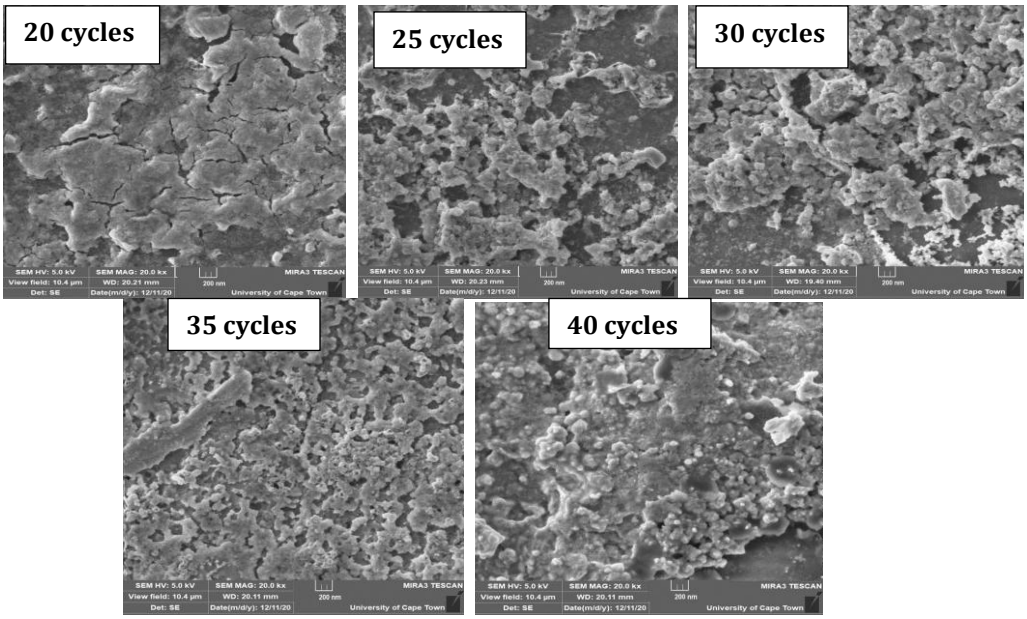

Figure 3: SEM micrograph of SnS/SnO material deposited at different deposition cycles

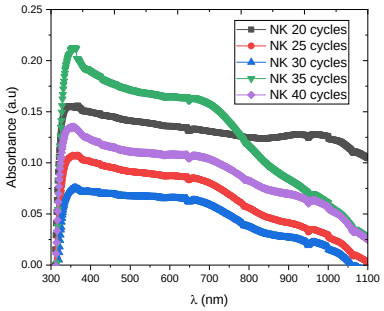

Figure 4:Plot of Absorbance against Wavelength for Different Cycles of SnS/SnO_2 Superlattice.

The absorbance of $SnS/SnO_2$is highest at a UV region and lowest at the infrared region. The absorbance decreases as wavelength increases with the highest absorbance at 35 Cycles to be 0.22. Also, as the SILAR cycle increases, the absorbance decreases.

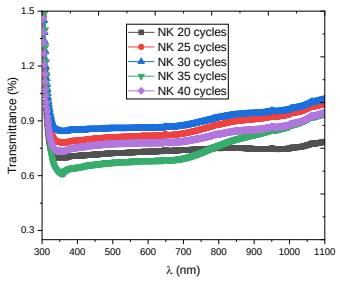

Figure 5 :Plot of Transmittance against Wavelenght for Different Cycles of SnS/SnO_2 Superlattice.
In the graph, Transmittance increases as wavelength increases with the highest transmittance at infrared region. Also, the graph shows that the transmittance decreases as number of SILAR cycles increases. From figure 5, with the highest transmittance at 30 SILAR cycles, it is observed that the transmittance is generally low.

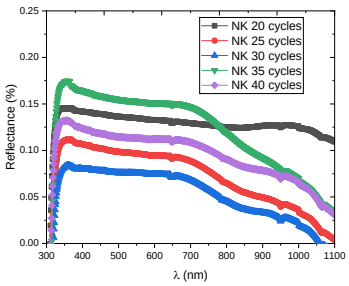

Figure 6:Plot of Reflectance against Wavelength for Different Cycles of SnS/SnO_2 Superlattice.
The graph of reflectance of the films plotted against the wavelength shows low reflectance generally. The reflectance reduces as wavelength increases. Also, as SILAR cycles decreases, the reflectance decreases and later increased, with highest at the UV region and lowest at the infrared region.

Table 2: **Variation of band gap of $SnS/SnO_2$with number of cycles**

Number of cycles	**Band gap (eV)**
20	3.35
25	2.75
30	3.01
35	2.75
40	3.00

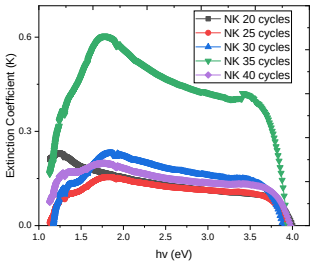

Figure 7:Plot of extension Coefficient against Wavelength for Different Cycles of SnS/SnO_2 Superlattice.

The graph of extension coefficient of the films plotted against wavelength is observed that as the SILAR cycles increases, the extension coefficient increases with its highest at the VIS region 400nm and is lowest at the infrared region 1100nm. The film deposited under 35 SILAR cycle as the highest extension coefficient at 0.61.

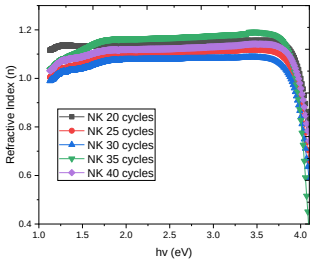

Figure 8: **Plot of Refractive Index against Wavelenght for Different Cycles of SnS/SnO_2 Superlattice.**

The films generally show low refractive index with highest refractive index at the NIR region. As the SILAR cycle increases the refractive index reduced and later increased.

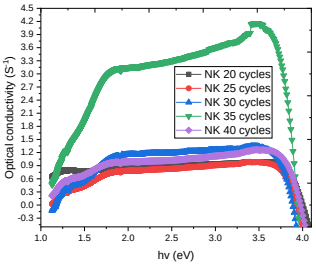

Figure 9 :**Plot of Optical Conductivity against Wavelength for Different Cycles of SnS/SnO_2 Superlattice.**

From the graph of optical conductivity against wavelength, it is observed that the films shows generally low optical conductivity with the highest Optical conductivity 4.2, under 35 SILAR cycles at NIR region.

CONCLUSION

In this study, SnS/SnO_2 heterojunction thin films were coated o glass surface, at the same room temperature using SILAR method in different number of cycles. The structural properties of SnS/SnO_2 thin films were investigated according to the number of cyclus, parameters were taken into consideration. The study showed that we could obtain better homogeneous and more crystalline films in a limited time by increasing the number of cycles in SnS/ SnO_2 thin films. Its concluded that SILAR method is a suitable method to enlarge the heterojunction thin films at SnS/ SnO_2, for solar energy application.

References:

[1] June John M. Vequizo and Masaya Ichimara (2012). Fabrication at electrodeposited $SnS/Sn0_2$ heterojunction solar cells. Japanese Journal of applied Physics 51 (2012) IONC38; 1-4

[2] Rama Krishna, Reddy N., and Miles R.W. (2006). Solar energy material. Solar cells 90. 325.

[3] Ristov M., Sinadinovski G., Mitreski M., and Ristova M. (2001) photovoltaic cells based on chemically deposited p.typeSnS solar energy materials and solar cells 69, 17-24.

[4] Raj, S,, Kumar, S., Srivastava, S. k., Kar, P and Poulomi Roy, P. (2018).Deposition of Tin Oxide Thin Films by successive Ionic Layer Adsorption Reaction Method and its Characterization . journal of Nanoscience and Nanotechnology, 18, 2569-2575.

[5] Zou, Y., Zhang, Y., Hu, Y. and Gu, H. (2018). Ultraviolet Detectors Based on Wide Bandgap Semiconductor Nanowire: A Review. Sensors, 18(2072); 1-25.